Constant gradient magnetic resonance elastography experiments on phantom and bovine liver.

Pilar Sango Solanas, Eric Reeth, Pauline Lefebvre, Hélène Ratiney, Elisabeth Brusseau, Denis Grenier, Steffen Glaser, Dominique Sugny, Olivier Beuf, Kevin Tse-Ve-Koon

HAL Id: hal-02142513
https://hal.archives-ouvertes.fr/hal-02142513

Submitted on 28 May 2019

Constant gradient magnetic resonance elastography experiments on phantom and bovine liver.

Pilar Sango Solanas[1], Eric Van Reeth[1], Pauline M. Lefebvre[2], Hélène Ratiney[1], Elisabeth Brusseau[1], Denis Grenier[1], Steffen J. Glaser[3], Dominique Sugny[4], Olivier Beuf[1], and Kevin Tse-Ve-Koon[1]

[1]Univ Lyon, INSA-Lyon, Université Claude Bernard Lyon 1, UJM-Saint Etienne, CNRS, Inserm, CREATIS UMR 5220, U1206, Lyon, France, [2]Université de Toulouse, CNRS, INPT, UPS, IMFT, Toulouse, France, [3]Department of Chemistry, Technische Universität München, Munich, Germany, [4]ICB, CNRS UMR6303, Université de Bourgogne, Dijon, France

Synopsis

Magnetic Resonance Elastography (MRE) is performed by the application of motion-sensitive gradients. In this study, RF pulses are designed with an optimal control algorithm to obtain a desired magnetization phase distribution. Such pulse, in presence of a constant gradient, allows to simultaneously perform spatially selective excitation and motion encoding. This offers some advantages when compared to standard MRE encoding strategy. Simulations, phantom and ex vivo experiments show that phase-to-noise ratios are improved. These results demonstrate that optimal control-based pulses can be used to encode motion in the MRE excitation phase with relevant advantages for further *in vivo* liver rat studies.

Introduction

MRE has become a valuable technique to quantify mechanical properties of tissues based on the characteristics of shear waves propagation. Conventionally, motion encoding gradients are applied between RF excitation and signal acquisition yielding phase images that depict the propagation of the shear wave[1]. The drawback of this technique is a longer echo-time and thus a degraded SNR. For that purpose, we propose to use a single RF excitation pulse that could simultaneously enable the slice selection and the motion encoding in the phase of the MR signal while also maximizing its norm. To this end, we use the optimal control (OC) formalism to design this RF pulse.

Methods

The application of optimal control theory to MRE consists in designing OC RF pulses which manipulate the magnetization ($\vec{M}$), whose evolution is governed by Bloch equations, towards a target state in which the isochromats phase is directly linked to the phase of the wave motion they are experiencing[2] while also taking into account the T2 so as to maximize the transverse magnetization. The OC pulse computation is performed with the GRAPE algorithm[3].

In the OC MRE strategy, the RF pulse is applied simultaneously with a constant gradient. This imposes slice selectivity[4] by considering isochromats located at different positions in the slice ($z^{(j)}$). Consequently to the application of the constant gradient G and sinusoidal shear wave motion at frequency f_e, static field variations experienced by an isochromat in position $\theta^{(i)}$ along the propagating shear wave and $z^{(j)}$ in the slice direction are given:

$$\Delta B_0^{(i,j)}(t) = G(A sin(-2\pi f_e t + \theta^{(i)}) + z^{(j)})$$

Different target states will be attributed whether an isochromat is located in (Δz_{in}) (the selected slice) or in (Δz_{out}), as illustrated in Fig. 1.

$$\vec{T}^{(i,j)} = \rho(Cos\Phi^i, Sin\Phi^i, 0) \ \ if \ \ j \in \Delta z_{in}$$

$$\vec{T}^{(i,j)} = (0,0,1) \ \ if \ \ j \in \Delta z_{out}$$

The defined cost function :

$$C = \sum_{j=1}^{J}\sum_{i=1}^{N} \| \vec{M}^{(i,j)}(t_f) - \vec{T}^{(i,j)} \|^2$$

requires minimizing the difference between final magnetization state ($\vec{M}^{(i,j)}$) and target state ($\vec{T}^{(i,j)}$) of the (i,j) spin ensemble.

The OC-MRE strategy was compared to standard MRE, through phantom and ex vivo MRE experiments. MRI measurements were run on a Bruker 4.7 T small-animal MRI-system, with a 70mm inner diameter volume coil. Shear waves were generated using a piezoelectric actuator (CEDRAT Technologies). Phantom experiments were carried out on a 100% plastisol (suspension of polyvinyl chloride particles in a liquid plasticizer) phantom5 whose relaxation times [T1, T2] = [300, 25] ms. Ex-vivo experiments were performed on a piece of bovine liver; relaxation times [T1, T2] = [650, 30] ms. The OC-pulse was optimized for an excitation frequency of 400Hz, a T2=20ms and a duration of 13.8ms. We used a RARE MRI sequence with parameters described in table 1. For the standard MRE, a conventional RARE MRE sequence was used, with an equal number of sinusoidal gradient periods (N_G = 2,4,6,8 for phantom and 2,4 for ex-vivo) before and after the refocusing pulse.

Results

Fig. 2. illustrates the B1 pulse magnitude obtained and the corresponding simulated and experimentally measured slice profiles demonstrating correct in-slice homogeneity and selectivity. Fig. 3. illustrates the phase images obtained on ex-vivo and phantom experiments. Fig. 4. compares phantom and ex vivo, standard and OC-MRE acquisitions. For standard acquisitions, increasing N_G increases the phase encoding (Δ) but decreases SNR. Computing a phase-to-noise ratio; PNR=$\Delta\times$SNR, accounts simultaneously for both. For phantom experiments, the OC-MRE produces good values of Δ while yielding the best SNR resulting in higher PNR. Furthermore, despite the difference between liver's T2 and the optimized T2, ex-vivo OC-MRE results show that OC-MRE still outperforms standard MRE.

Conclusion and Discussion

A new encoding strategy of the shear wave propagation, by simultaneously applying a tailored RF pulse and a constant gradient was demonstrated. The RF pulse, which simultaneously performs frequency selective excitation and motion encoding thus allows extremely short echo times. Phantom and ex-vivo measurements demonstrate the ability of the OC-pulse to outperform standard MRE even when T2 values are different from the optimized one (which would have been a limiting factor for future applications). Future work will focus on investigating multi-frequency excitation and pre-clinical in vivo studies on rat livers will be conducted to evaluate the encoding improvement of OC MRE.

Acknowledgements

References

1. Muthupillai R, Lomas D, Rossman P, Greenleaf J, Manduca A, Ehman R. Magnetic resonance elastography by direct visualization of propagating acoustic strain waves. *Science* 1995; 269:1854–1857.

2. Lefebvre PM, Van Reeth E, Ratiney H, et al. Active control of the spatial MRI phase distribution with optimal control theory. *Journal of Magnetic Resonance* 2017; 281:82–93.

3. Khaneja N, Reiss T, Kehlet C, Schulte-Herbrüggen T, Glaser SJ. Optimal control of coupled spin dynamics: design of NMR pulse sequences by gradient ascent algorithms. *Journal of Magnetic Resonance* 2005; 172:296–305.

4. Vinding MS, Maximov II, Tošner Z, Nielsen NC. Fast numerical design of spatial-selective rf pulses in MRI using Krotov and quasi-Newton based optimal control methods. *The Journal of Chemical Physics* 2012; 137:054203.

5. Lefebvre PM, Tse Ve Koon K, Brusseau E, et al. Comparison of viscoelastic property characterization of plastisol phantoms with magnetic resonance elastography and high-frequency rheometry. In *2016 38th Annual International Conference of the IEEE Engineering in Medicine and Biology Society (EMBC)*. Orlando, FL, USA: IEEE; 2016:1216–1219.
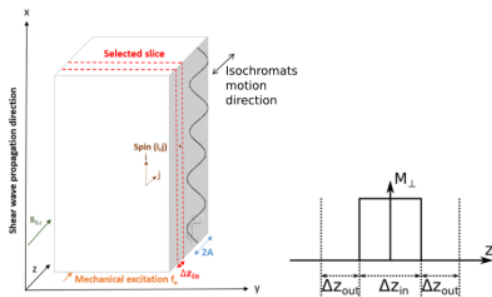
Figures

Figure 1. At left: experimental setup: the shear wave, of f_e mechanical excitation frequency, propagates (amplitude A) in the phantom along the x axis. The shear wave-dephasing angle is defined as $\theta^{(i)} = 2\pi x^{(i)}/\lambda$ with $x^{(i)}$ representing a specific position. At right: Ideal slice profile.
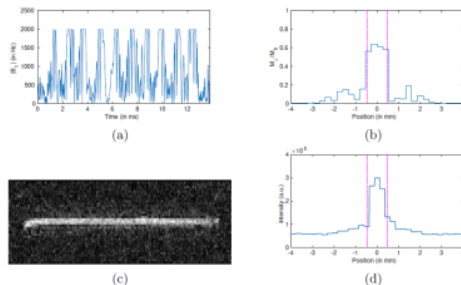

Figure 2. (a) Magnitude of the optimized RF pulse. (b) Simulated slice profile. (c) Acquired slice profile of the *ex vivo* experiment. (d) Averaged slice profile. Dotted lines indicate the theoretical slice thickness.
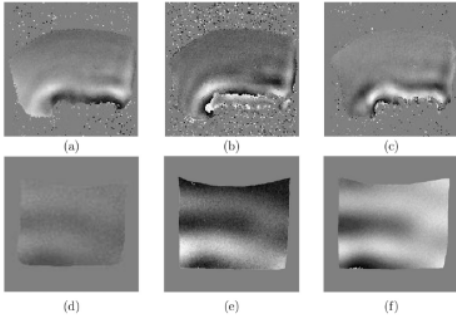
Figure 3. (a)-(c) Unwrapped phase images of the ex vivo experiment obtained with (a) the standard MRE with 2 encoding periods, (b) 4 encoding periods, and (c) the OC MRE scheme. (d)-(f) Unwrapped masked phase images of the in vitro experiment obtained with (d) standard MRE with 2 encoding periods, (e) 6 encoding periods, and (f) the OC MRE scheme.
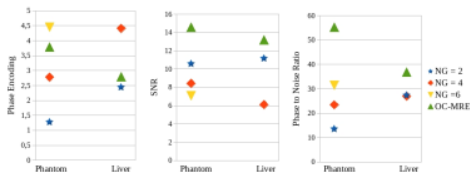

Figure 4. Comparison between the OC MRE and standard MRE schemes of different encoding periods numbers (NG) for both phantom and ex vivo experiments (liver sample). (a) phase amplitude variation (), (b) signal-to-noise ratio (SNR) and (c)phase-to-noise ratio (PNR) along a line going through the wave propagation pattern.

	Phantom		Liver	
	Standard MRE	OC-MRE	Standard MRE	OC-MRE
TR (ms)	1500	1500	2000	2000
FOV (cm²)	3.5×3.5	3.5×3.5	5.5×2.5	5.5×2.5
Matrix	128×128	128×128	128×128	128×128
Slice Thickness (mm)	0.93	0.93	0.93	0.93
Turbo factor	2	2	4	4
NA	1	1	2	2

Table 1. Acquisition parameters of standard and OC-MRE experiments carried out on phantom and liver.